Journal of *Marine Science and Engineering*

MDPI

Article

Increase in Stability of an X-Configured AUV through Hydrodynamic Design Iterations with the Definition of a New Stability Index to Include Effect of Gravity

Lakshmi Miller [1,*], Stefano Brizzolara [1] and Daniel J. Stilwell [2]

[1] Kevin Crofton Department of Aerospace and Ocean Engineering, Virginia Tech, Blacksburg, VA 24060, USA; stebriz@vt.edu
[2] The Bradley Department of Electrical and Computer Engineering, Virginia Tech, Blacksburg, VA 24060, USA; stilwell@vt.edu
* Correspondence: lakshmimiller@vt.edu

Abstract: A study about the effect of different configurations of stationary and movable appendages on the dynamic stability of an autonomous underwater vehicle (AUV) is presented. A new stability index that can be used to assess dynamic stability in the vertical plane is derived. It improves upon the vertical plane stability index by accurately accounting for the contribution of hydrostatic forces to dynamic stability, even at low speeds. The use of the new stability index is illustrated by applying it to a set of AUV configurations based on an AUV initially designed at Virginia Tech and built by Dive Technologies. The applicability of this index depends on the speed of the craft. The range of applicability in terms of speed is presented for the DIVE craft as an example. The baseline design of the DIVE craft has asymmetry in the vertical plane and symmetry in the horizontal plane. A virtual planar motion mechanism (VPMM) is used to obtain the hydrodynamic coefficients of the hull. Design iterations are performed on the baseline design by varying the appendages in shape and size, adding appendages and adding features on appendages. The best and the baseline design from this effort are incorporated in a 6 DOF lumped-parameter model (LPM) to compare results of a straight line maneuver. A computational fluid dynamic (CFD) tool is used to obtain the trajectory comparison of turn-circle maneuver for these two designs. A principal conclusion is the important contribution of a hydrostatic restoring force at low-moderate speeds by using $G_{V grav}$ and the influence of design of control surfaces, both stationary and non-stationary, in the achievement of control-fixed course stability.

Keywords: hydrodynamics; maneuvering; stability; shape optimization; design; stability index; hydrostatic moment; hydrostatic force; AUV; underwater vehicles

Citation: Miller, L.; Brizzolara, S.; Stilwell, D.J. Increase in Stability of an X-Configured AUV through Hydrodynamic Design Iterations with the Definition of a New Stability Index to Include Effect of Gravity. *J. Mar. Sci. Eng.* **2021**, *9*, 942. https://doi.org/10.3390/jmse9090942

Academic Editor: Weicheng Cui

Received: 1 August 2021
Accepted: 16 August 2021
Published: 30 August 2021

1. Introduction

The design of an AUV and its control surfaces have an important role to play in the maneuverability and stability of a craft. Minnick [1] has developed a stability and control module to determine the hydrodynamic derivatives and stability characteristics of a craft. We explore the definition of stability using hydrodynamic derivatives to include the effect of gravity. The report of Sweat [2] shows that any conventional torpedo hull form, when designed to meet certain design criteria that indicate feedback gain and effective tail fin size through hydrodynamic parameters, shall exhibit similar step response characteristics in the presence of a proportional controller. We investigate the increase in hydrodynamic stability with design changes.

Lambert [3] investigated the effect of change in first order stability derivatives on the dynamic behavior of a torpedo hull. A torpedo is said to have linear dynamic stability if sway or pitch returns to zero after a disturbance from a linear path. The stability inequality derived in Lambert [3] is similar to the dynamic stability defined in Section 4.2

of in Lewis et al. [4], and both do not address the effect of gravity. The stability parameter G [5] (defined in Table 1) is further used to classify the craft as unstable, marginally stable, or dynamically stable. The three aspects of dynamic behavior investigated by Lambert [3] are turning circle radius, value of G, and the transient motion following a disturbance from an originally linear path in the vertical plane. The systematic analysis highlights the effect of hydrodynamic derivatives on the stability index, much like the discussion presented in this article. Lambert [3] studied the effect of stability variations on torpedo control. We study the stability of the craft with and without gravity to illustrate the increase in stability using turning circle and straight line maneuvers.

Table 1. Definitions of various symbols and abbreviations used in this document.

Index	Definition
G	stability criterion by Roddy [6]
G_V	stability parameter traditionally defined for the vertical plane of submarines
G_{Vgrav}	stability parameter defined in this article accounting for hydrostatic force
N'_v, N'_r	non-dimensionalized first order derivative of yaw moment with respect to sway (v) and yaw (r) rate, respectively
M'_w, M'_q	non-dimensionalized first order derivative of yaw moment with respect to heave (w) and pitch (q) rate, respectively
Y'_v, Y'_r	non-dimensionalized first order derivative of sway force with respect to sway (v) and yaw (r) rate, respectively
Z'_w, Z'_q	non-dimensionalized first order derivative of heave force with respect to heave (w) and pitch (q) rate, respectively
m'	non-dimensionalized mass
u, v, w	velocity components along x, y and z axes in the body reference frame
$\dot{u}, \dot{v}, \dot{w}$	acceleration components along x, y and z axes in the body reference frame (BRF)
x_G, y_G, z_G	coordinates of center of gravity
X, Y, Z	external components of force acting on the craft
K, M, N	external moments acting on the craft about the COG
p, q, r	rotation rate about the roll (x), pitch (y), and yaw (z) axes, respectively
$\dot{p}, \dot{q}, \dot{r}$	angular acceleration about roll (x), pitch (y), and yaw (z) axes, respectively
$C_B C_G$	vertical distance from COB to COG
COG	center of gravity
COB	center of buoyancy
NP	neutral point
CP	critical point
g	acceleration due to gravity
C_d	coefficient of drag
I_{axax}	mass moment of inertia with respect to specified axes 'ax' and 'ax'
A, B, C	coefficients of characteristic polynomial
σ	variable of characteristic polynomial

The impact of dimensional characteristics on stability is further addressed in the work of Roddy [6] which is experimental in nature. Roddy [6] shows that hydrodynamic coefficients can be derived experimentally through virtual planar motion mechanism (VPMM) tests and that the resulting conventional stability indices G_H and G_V (Renilson [7]) can be compared for stability of design iterations. In the case of the DARPA sub-off model, stability indices corresponding to the presence and absence of appendages are derived and compared. The expression used for the stability index in the vertical plane is the same as shown in Renilson [7] but with the origin of the craft offset from the COG. We note that the effects of gravity on stability are not addressed in Lambert [3] or Lewis et al. [4]. The work of Lambert [3] addresses vertical plane motion but considers fast-moving torpedoes for which the effect of gravity is negligible, while Lewis et al. [4] considers yaw-axis stability of ships and has no reason to consider vertical plane stability.

Park et al. [8] included changes in the configuration of appendages and based stability calculations on revised equations from Feldman [9]. The purpose was to understand the effects of the various appendages on hydrodynamic coefficients and stability. The

expression for G_V remained equivalent to Renilson [7]. We study the effect of appendages through the newly defined stability index in comparison to the traditional stability index.

We build upon previous work such as Lewis et al. [4], Renilson [7], and Fossen [10] on assessing the stability of a family of vessel shapes by developing a new vertical plane coefficient that accurately accounts for the effects of hydrostatic forces. The stability indices for the horizontal and vertical plane as well as the new stability index for the vertical plane are defined in terms of hydrodynamic coefficients. High fidelity Reynolds-averaged Navier–Stokes equations (RANSE) simulations are used to obtain hydrodynamic coefficients to enable the comparison of various design iterations for stability. Computational fluid dynamics (CFD) has been used as an alternative to experimental planar motion mechanism (PMM) in research works such as Coe and Neu [11]. Cho et al. [12] investigates the derivation of hydrodynamic coefficients for a submarine with X configuration of control surfaces. Cho et al. [12] indicates the reliability of hydrodynamic coefficients obtained using CFD data by comparing them with experimental data.

The stability indices are used in a lumped-parameter model (LPM) to simulate a maneuver in the vertical plane. Time-accurate unsteady RANSE simulations are performed for turning circle maneuvers to validate the observations from an LPM. The primary aim is to demonstrate an increase in the stability of the craft in the vertical plane, calculate the corresponding stability index, and show that the change in stability is validated upon implementation in LPM and/or CFD. Our analysis highlights the importance of accounting for hydrostatic force when assessing stability at low to moderate speeds.

2. Stability Indices

The equations of motion for a submersible craft based on Newton's second law are written in the body reference frame (BRF) with a generic origin as shown in Figure 1. The forces X, Y, and Z corresponding to surge, sway, and roll, respectively, satisfy

$$X = m\left[\dot{u} - vr + wq - x_G\left(q^2 + r^2\right) + y_G(pq - \dot{r}) + z_G(pr + \dot{q})\right] \quad (1)$$

$$Y = m\left[\dot{v} - wp + ur + x_G(qp + \dot{r}) - y_G\left(r^2 + p^2\right) + z_G(qr - \dot{p})\right] \quad (2)$$

$$Z = m\left[\dot{w} - uq + vp + x_G(rp - \dot{q}) + y_G(rq + \dot{p}) - z_G\left(p^2 + q^2\right)\right] \quad (3)$$

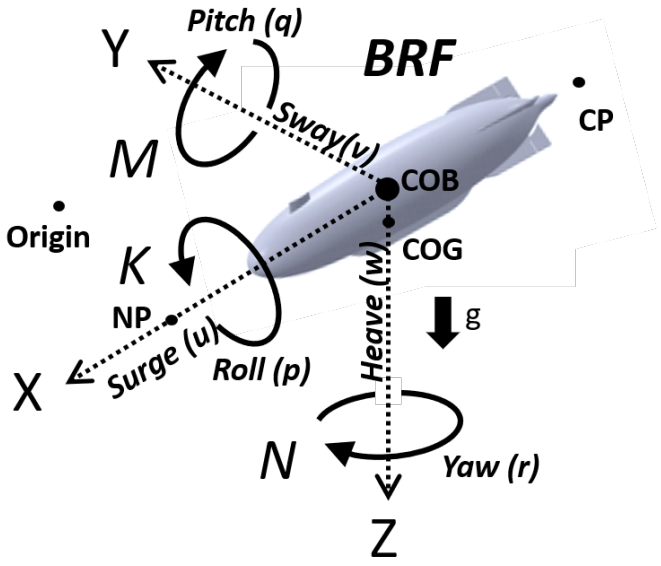

Figure 1. Reference for body frame and world frame coordinate system used in this document.

The moments, K, M, and N corresponding to roll, pitch, and yaw, respectively, satisfy

$$\begin{aligned} K = {} & I_{xx}\dot{p} + \left(I_{zz} - I_{yy}\right)qr - (\dot{r} + pq)I_{zx} \\ & + \left(r^2 - q^2\right)I_{yz} + (pr - \dot{q})I_{xy} \\ & + m[y_G(\dot{w} - uq + vp) - z_G(\dot{v} - wp + ur)] \end{aligned} \tag{4}$$

$$\begin{aligned} M = {} & I_{yy}\dot{q} + (I_{xx} - I_{zz})rp - (\dot{p} + qr)I_{xy} \\ & + \left(p^2 - r^2\right)I_{zx} + (qp - \dot{r})I_{yz} \\ & - m[x_G(\dot{w} - uq + vp) - z_G(\dot{u} - vr + wq)] \end{aligned} \tag{5}$$

$$\begin{aligned} N = {} & I_{zz}\dot{r} + \left(I_{yy} - I_{xx}\right)pq - (\dot{q} + rp)I_{yz} \\ & + \left(q^2 - p^2\right)I_{xy} + (rq - \dot{p})I_{zx} \\ & + m[x_G(\dot{v} - wp + ur) - y_G(\dot{u} - vr + wq)] \end{aligned} \tag{6}$$

The external forces (X, Y, Z) and moments (K, M, N) are obtained by adding components that are hydrodynamic or hydrostatic in nature. The components of the forces obtained due to motion of the craft or its control surfaces are hydrodynamic, whereas the components of the force obtained due to the weight and buoyancy of the craft are hydrostatic in nature. The hydrodynamic forces on the hull, which are a function of the velocity and acceleration of the body, are expanded in a Taylor series with respect to the velocity and acceleration components around a reference dynamic equilibrium state (e.g., Feldman [9]). The sway force, yawing moment, and surge force are expanded up to the second order in terms of u, v, and r, while the heave force, rolling, and pitching moments are expanded up to second order in terms of w, p, and q.

2.1. Controls Fixed Linear Dynamic Stability Index for the Horizontal Plane

The origin of the coordinate system is assumed to be at COB for the ease of calculations in this section. The COG is assumed in the same vertical axis beneath the COB for stability of the craft. Port/starboard symmetry is assumed for the purpose of derivation of the expressions for stability. The velocity, displacement, and acceleration in the vertical plane are set to zero. The craft moving at a constant forward speed results in a zero acceleration in surge. The horizontal plane stability index is derived from the equations of motion in the horizontal plane as

$$G_H = 1 - N'_v(Y'_r - m')/[Y'_v N'_r] \tag{7}$$

2.2. Controls Fixed Linear Dynamic Stability Index for the Vertical Plane

The vertical plane expression for stability is usually derived by assuming high speeds and therefore neglecting effects of hydrostatic force and moment (e.g., Renilson [7], Lewis et al. [4], Lewandowski [13]). The derivation below shows the method of inclusion of these effects for AUVs and gliders of low-moderate speeds. The vertical plane equations for control-fixed stability as shown in Spencer [14] are

$$\begin{aligned} & \left(m' - Z'_{\dot{w}}\right)\dot{w}' - w'Z'_w - \left(m' + Z'_q\right)q' = 0 \\ & \left(I'_y - M'_{\dot{q}}\right)\dot{q}' - w'M'_w - q'M_q{}' + m'\gamma\int q'd\tau = 0 \end{aligned} \tag{8}$$

where

$$\begin{aligned} \gamma &= \frac{g\,BG}{u^2} \\ q' &= \frac{\left(m' - Z'_{\dot{w}}\right)\dot{w}' - w'Z'_w}{\left(m' + Z'_q\right)} \end{aligned} \tag{9}$$

$$\dot{q}' = \frac{(m' - Z'_{\dot{w}})\dot{w}' - \dot{w}' Z'_w}{\left(m' + Z'_q\right)} \tag{10}$$

Substituting (9) and (10) in (8) and multiplying by $\left(m' + Z'_q\right)$, we have a third order differential equation written as

$$\begin{gathered}(m' - Z'_{\dot{w}})\left(I'_y - M'_{\dot{q}}\right)\dddot{f}(\tau) \\ -\left[M'_q(m' - Z'_{\dot{w}}) + Z'_w\left(l'_y - M'_{\dot{q}}\right)\right]\ddot{f}(\tau) \\ +[Z'_{\dot{w}}M'_q - M'_w\left(m' + Z'_q\right) + m'\gamma(m' - Z'_{\dot{w}})]\dot{f}(\tau) \\ -m'\gamma Z'_w f(\tau) = 0\end{gathered} \tag{11}$$

where

$$f(\tau) = \int w' d\tau \tag{12}$$

The solution is of the form

$$\begin{gathered}w' = a_1 e^{\sigma_1 \tau} + a_2 e^{\sigma_2 \tau} + a_3 e^{\sigma_3 \tau} \\ q' = b_1 e^{\sigma_1 \tau} + b_2 e^{\sigma_2 \tau} + b_3 e^{\sigma_3 \tau}\end{gathered} \tag{13}$$

where σ_1, σ_2 and σ_3 are the roots of the characteristic equation

$$A\sigma^3 + B\sigma^2 + C\sigma + D = 0 \tag{14}$$

Hence, the coefficients are

$$\begin{gathered}A = (m' - Z'_{\dot{w}})\left(I'_y - M'_{\dot{q}}\right) \\ B = -\left[M'_q(m' - Z'_{\dot{w}}) + Z'_w\left(l'_y - M_{\dot{q}}{}'\right)\right] \\ C = Z'_w M'_q - M'_w\left(m' + Z'_q\right) + m'\gamma(m' - Z'_{\dot{w}}) \\ D = -m'\gamma Z'_w\end{gathered} \tag{15}$$

Coefficient A is positive because it is the product of added mass and added inertia, which are necessarily positive. Thus, the direct application of the Routh–Hurwitz criteria (see Ogata [15]) applied to (Equation (16)) shows that

$$B > 0; D > 0; BC > AD \tag{16}$$

becomes sufficient for (14) to be stable. Coefficient B is always positive since the damping coefficients Z'_w and $M_q{}'$ are negative. Coefficient D is positive when γ is positive. Upon expansion of the terms BC and AD,

$$BC = K + AD \tag{17}$$

where

$$\begin{gathered}K = -M'_q Z'_w M'_q(m' - Z'_{\dot{w}}) + M'_q M'_w(m' - Z'_{\dot{w}})\left(m' + Z'_{\dot{q}}\right) \\ -m'\gamma M'_q(m' - Z'_{\dot{w}})^2 - Z'^2_w M_q\left(I_y{}' - M'_{\dot{q}}\right) \\ +Z'_w M'_w\left(I_y{}' - M'_{\dot{q}}\right)\left(m' + Z'_{\dot{q}}\right)'\end{gathered} \tag{18}$$

A force on the craft in the vertical plane results in a moment of the same sign. A force on the craft in the horizontal plane results in a moment in the opposite direction. Since Z'_w and M'_q are always negative, M'_w is positive (based on the sign conventions in Figure 1). Added mass and added inertia are positive by nature. The first three terms in

the expression for K in (18) are positive. The fourth and fifth terms in K shall be positive only if C is positive. Therefore, the condition for stability becomes

$$C > 0 \tag{19}$$

For a hydrostatically stable craft, γ and $C_B C_G$ are always positive. From (15) and (19),

$$Z'_w M'_q - M'_w\left(m' + Z'_q\right) + m'\gamma\left(m' - Z'_{\dot{w}}\right) > 0$$

$$1 - \frac{M'_w\left(m' + Z'_q\right)}{Z'_w M'_q} + \frac{m'\gamma(m' - Z'_{\dot{w}})}{Z'_w M'_q} > 0 \tag{20}$$

At faster speeds where u is large, γ becomes negligible, producing the traditional definition of the vertical plane stability index

$$G_V = 1 - M'_w(Z'_q + m')/[Z'_w M'_q] \tag{21}$$

Feldman [5] shows that the craft is stable for positive values of G_V as shown in Table 2, is marginally stable for the range 0–0.2, has good dynamic performance for 0.2–0.7, and is highly stable for values greater than 0.8. The work of Bottacini [16] (page 45) shows the meaning of the margin of stability using experimentally calculated coefficients for torpedos with aft-mounted stabilizers and rudders. These ranges can be understood in terms of the restoring moment experienced by the craft when perturbed from its initial condition. The stability index in the vertical plane signifies the ratio of the rotational motion due to pitch with respect to the rotational motion due to heave. A larger magnitude of this ratio results in the craft returning to the origin faster. Substituting the definition of G_V from (21), the expression for C is further reduced without neglecting hydrostatic effects for low to moderate speeds.

$$G_V + \frac{m'\gamma(m' - Z'_{\dot{w}})}{Z'_w M'_q} > 0 \tag{22}$$

$$G_{Vgrav} := G_V + \frac{m'\gamma(m' - Z'_{\dot{w}})}{Z'_w M'_q} \tag{23}$$

Equation (22) is the stability inequality to be satisfied for all speeds, including low-moderate speeds, for the linear dynamic stability of submerged craft. The right-most term in Equation (23) that adds on to the traditional definition of G_V shall always be a positive quantity due to the nature of the contributing coefficients. Therefore, the stability of the craft may be underestimated at low-moderate speeds with the use of G_V. The range of applicability of G_{Vgrav} for the DIVE craft at various speeds and $C_B C_G$ separations is given in Table 3.

Table 2 shows the recommended range of G_H for stability, with the recommended value being 0.2 as indicated by Feldman [5]. A positive value of the stability index implies that the ratio of the rotational motion due to yaw and the rotational force has to be greater than the ratio of the rotational motion due to sway and the sway force. In other words, the moment arm of the rotational motion due to yaw must be greater than that of the rotational motion due to sway. The captive model experiments used to determine the range of G_V would still hold true for the new index Feldman [5].

Table 2. The range recommended for G_H by Renilson [7] and G_V by Feldman [5].

Index	Recommended Range
G_H	0.2 to 0.4
G_V	0 to 0.8

Table 3. Ratio $(G_{V_{grav}} - G_V)/G_V$ is an expressed percent to indicate the significance of the new index with respect to speed and C_BC_G separation. The first column is forward speed non-dimensionalized as Froude number; the first row is C_BC_G non-dimensionalized with craft diameter. The green areas (bold font) are applicable for the assumption of high speed, i.e., these areas have negligible difference if gravity is considered. The white areas (regular font) can go either way depending on required accuracy of linear dynamic stability. The red areas (italic font) are recommended for the implementation of $G_{V_{grav}}$. This implies that the inclusion of gravity has a significant effect on the value of stability index. The range of applicability would obviously change with the design of craft. These values are presented for the baseline design and shall apply to all the iterations presented.

C_BC_G/D Fr No.	0.028	0.03	0.04	0.05	0.06	0.07	0.08
0.137	*26*	*39*	*52*	*65*	*78*	*91*	*104*
0.27	*7*	*10*	*13*	*16*	*20*	*23*	*26*
0.41	*3*	*4*	*6*	*7*	*9*	*10*	*12*
0.55	2	2	*3*	*4*	*5*	*6*	*7*
0.69	1	2	2	*3*	*3*	*4*	*4*
0.82	**1**	1	1	2	2	*3*	*3*
0.96	**1**	**1**	1	1	2	2	2
1.10	**0**	**1**	**1**	1	1	1	2
1.24	**0**	**0**	**1**	**1**	**1**	1	1
1.37	**0**	**0**	**1**	**1**	**1**	**1**	1
1.51	**0**	**0**	**0**	**1**	**1**	**1**	**1**
1.65	**0**	**0**	**0**	**0**	**1**	**1**	**1**
1.78	**0**	**0**	**0**	**0**	**0**	**1**	**1**
1.92	**0**	**0**	**0**	**0**	**0**	**0**	**1**
2.06	**0**	**0**	**0**	**0**	**0**	**0**	**0**
2.20	**0**	**0**	**0**	**0**	**0**	**0**	**0**
2.33	**0**	**0**	**0**	**0**	**0**	**0**	**0**
2.47	**0**	**0**	**0**	**0**	**0**	**0**	**0**
2.61	**0**	**0**	**0**	**0**	**0**	**0**	**0**
2.75	**0**	**0**	**0**	**0**	**0**	**0**	**0**

Both G_V and $G_{V_{grav}}$ contain the non-dimensionalized definition of the position of the neutral point (NP) as defined by Spencer [14]. The NP is the point at which the submersible craft can experience a vertical force and result in a change of depth without trimming (24).

$$x_{NP} = -L\frac{M'_w}{Z'_w} \tag{24}$$

The importance of the NP for the inequality of stability is discussed in Spencer [14]. The critical point (CP) is discussed for the effect on maneuvering due to the position of the appendages by Spencer [14]. The CP is the point at which the craft can experience a force that leads to trim without a resultant change in depth(25).

$$x_{CP} = -L\frac{M'_w}{Z'_w} + \frac{gm'(C_BC_G)}{uZ_w} \tag{25}$$

While the non-dimensionalized NP is included in the definition of the stability index G_V, the CP is not, as seen from (21) and (23). This leads us to wonder if the inclusion of the hydrostatic force term results in encompassing the definition of non-dimensionalized CP within the stability index in (23). The inclusion of the definition of CP indicates that the position and effectiveness of stern appendages play an important role in the stability of the craft. The hydrostatic restoring force term, originally not included as explained in Minnick [1], at low speed becomes important for judging the effect of the control surfaces on the stability of the craft. The effect is further highlighted by the data presented here. While it is true that the hydrostatic force or restoring moment is dependent on speed,

when design changes affect the vertical plane stability, there is justification for including it as part of the stability index to reflect mass and appendage design variation at low-moderate speeds.

3. CFD Simulations

All fully viscous CFDs were performed in StarCCM+ version 13.03.11 RANSE solver. The space between the control fins of the craft and the hull form was extruded and filled to enable better meshing characteristics. Since there is no relative motion between the control surfaces and the hull in the simulations below, the approximation was acceptable. The simulations that are used in this document are of two types:

1. Planar motion mechanism;
2. Turn-circle maneuver.

The CFD setups of each of the above type of simulation are different. The steady drift simulations are steady state and use a simple domain with the craft being stationary with an angle of the inflow with respect to the axis of the craft. The VPMM simulations involve following a prescribed yaw/sway or pitch/heave forced maneuver by means of an overset mesh moving with the craft over a background mesh. These result in efficiency of computation with craft characteristics obtained in 6 degrees of freedom. The turn-circle maneuver is an unsteady simulation with the craft in a well-sized domain to enable capturing the accurate trajectory of a craft with deflected fins.

3.1. Planar Motion Mechanism

The simulations in CFD are performed for the standard VPMM tests for sway, yaw, heave, pitch, surge, and roll. These simulations are similar to those outlined by Coe and Neu [11]. An overset mesh with dynamic fluid body interaction motion [DFBI] was used. The moving region was of 9.48 million polyhedral cells, while the stationary region was of 34 M. A cylindrical volume control of 6.5 L length and 0.6 L was placed, encompassing the body to refine it further. The stationary domain is a cylinder of length 9 L and radius L. The overlapping region is a cuboid of dimensions 1.41 L $\times$ 0.51 L $\times$ 0.51 L. This simulation is unsteady and implicit with a 6 DOF motion solver.

The simulation was run for 4.5 s of physical time, but only the last of the three periods of the maneuver is used in the processing to ensure the converged data illustrated in Figure 2. The k-ϵ turbulence model was used. Inner iterations were set at a maximum of 5. The frequency of 0.667 Hz is chosen based on Coe and Neu [11], and amplitudes of 6 cm and 3 cm are chosen for obtaining a comprehensive dataset. The primary outputs are craft orientation, velocity, acceleration, forces and moments in the world, and body reference frames. The simulations are split into two types: vertical plane and horizontal plane. For the craft used in this study, the asymmetry makes the vertical plane more significant for stability. Vertical plane simulations were run for all the design iterations considered, whereas the horizontal plane simulations were run for the baseline and best designs to ensure comprehensive and time efficient evaluation. The vertical plane coefficients M_{ww}, M_{uw}, $M_{\dot{w}}$, Z_{ww}, Z_{uw}, $Z_{\dot{w}}$ from heave, M_{qq}, M_{uq}, $M_{\dot{q}}$, Z_{qq}, Z_{uq}, and $Z_{\dot{q}}$ are obtained by identification Njaka et al. [17] from the time histories of the heave force (Figure 3) and pitch (Figure 4) moment measured during the simulated captive maneuvers. Similarly, sway and yaw simulations result in the coefficients Y_{uv}, Y_{vv}, $Y_{\dot{v}}$, N_{uv}, N_{vv}, $N_{\dot{v}}$, N_{rr}, N_{ur}, $N_{\dot{r}}$ Y_{rr}, Y_{ur}, and $Y_{\dot{r}}$.

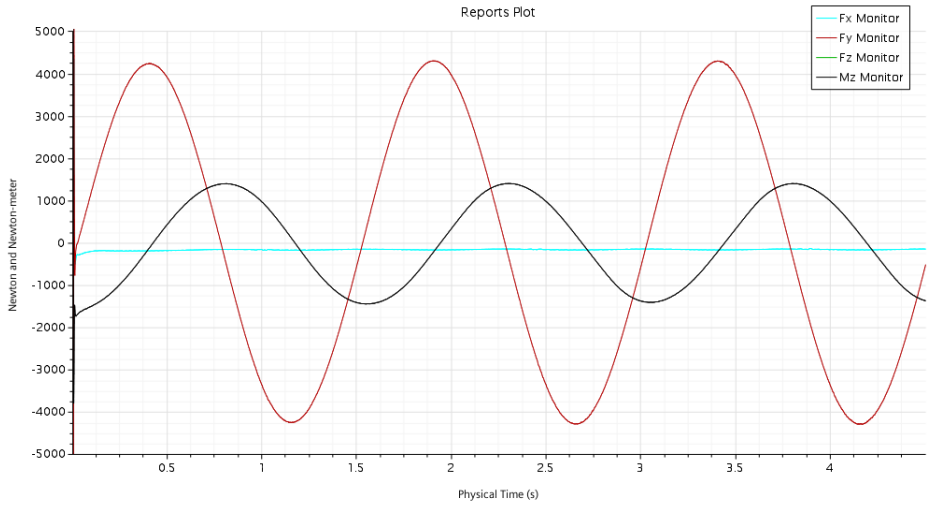

Figure 2. Sway force and yaw moment time history recorded during a virtual planar motion mechanism run.

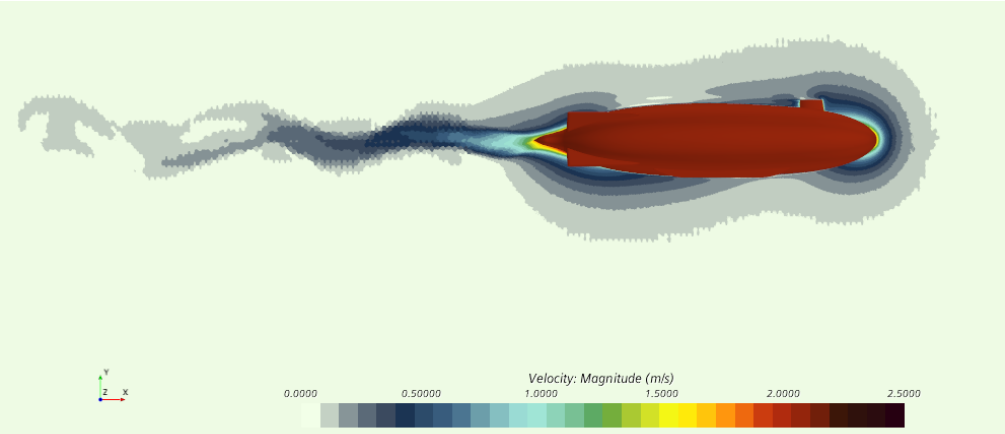

Figure 3. Velocity contour of pure heave maneuver from CFD.

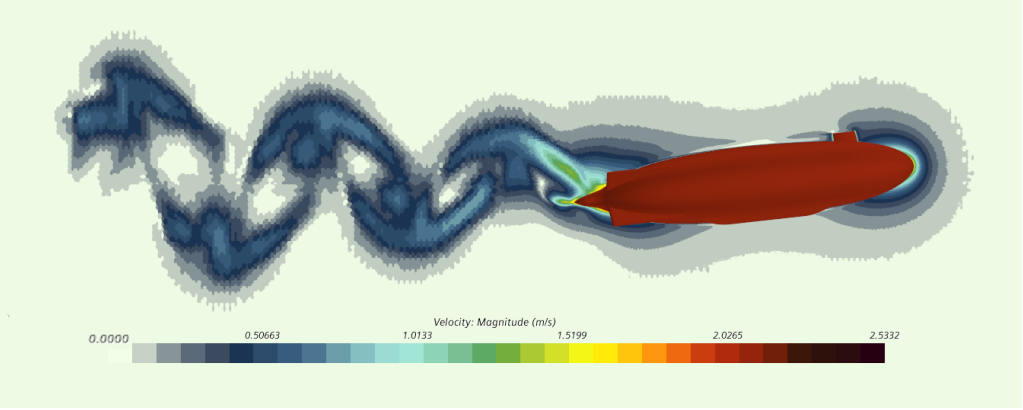

Figure 4. Velocity contour of pure pitch maneuver from CFD.

3.2. Turning Circle Maneuver

The turning circle simulations use a DFBI overset mesh as well. The solver is implicit and unsteady with a physical time of 200 s and maximum inner iterations of 10. The mesh consists of 51 million cells with a cylindrical domain of 1.5 L and radius 0.1 L. The output of these simulations, namely orientation, rotation, and translation help in obtaining the trajectory of the turning circle and hence the radius. The craft has deflected fins from the

start in these simulations. The motion of the craft is constrained to the horizontal plane. These simulations were performed for the baseline and final design iterations only.

4. Baseline Design

The craft consists of a hull appended with a small sail and two skates (bilge keels). The purpose of the sail is to house electronics. The skates are a unique feature of the DIVE craft, shown in Figure 1 and Table 4, serving the purpose of supporting the craft when placed on land. The control surfaces include fixed fins called strakes and control fins that are movable. The fins are designed in an 'X' configuration. Dubbioso et al. [18] shows that the X configuration of fins produces a superior level of turning ability in a submarine when compared to a cross configuration of fins. The configuration also ensures drag efficiency and absence of control surfaces directly behind the sail. The primary intent of the axisymmetric hull is drag optimization at 4 kn. The principal characteristics of the fully appended hull are shown in Table 5. For the purpose of stability, the craft is symmetric in the horizontal plane and asymmetric in the vertical plane.

Table 4. Design iterations and their descriptions.

Design Number	CAD Image	Description
Design 1	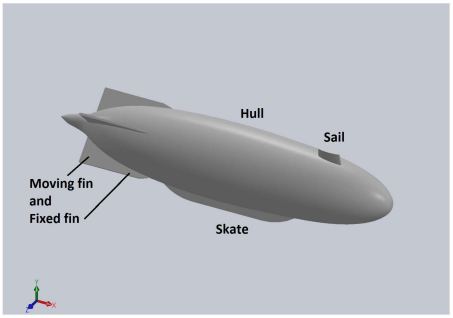 Baseline model	Baseline model: fully appended. The socket gap between control fins and fixed strakes is filled for CFD.
Design 2	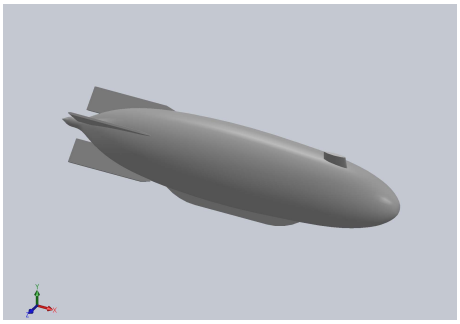 Extended Strakes model	Extended strakes model: The control fins are extended lengthwise.
Design 3	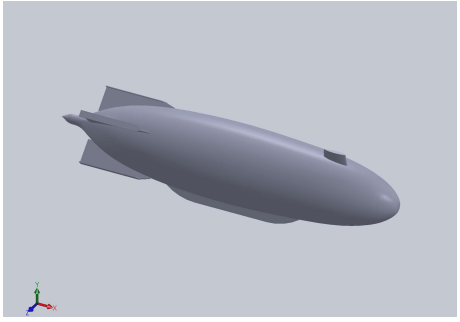 T-Strakes model	T-strakes model: The control fins and fixed strakes are appended with a T at the edges to increase fin surface area.

Table 4. *Cont.*

Design Number	CAD Image	Description
Design 4	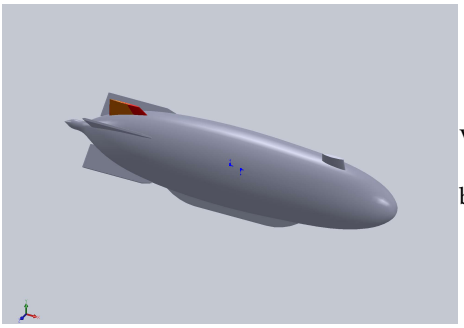 Vertical Fins model	Vertical Fins model: A vertical fin that is fixed, in addition to the four strakes, is added to the stern of the craft at the top and bottom. The added fins follow a NACA profile to minimize drag.
Design 5	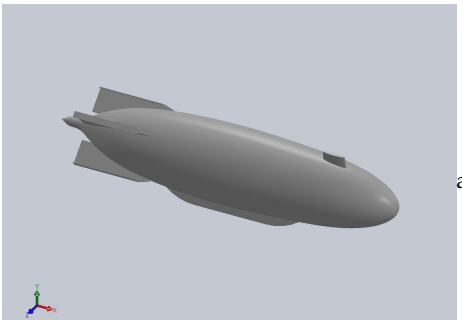 Hybrid Narrow model	Hybrid narrow model: The fins are extended and have a T-shaped edge, making this model a combination of Designs 2 and 3. The T-shaped edge has a triangular leading edge to avoid stagnation.
Design 5a	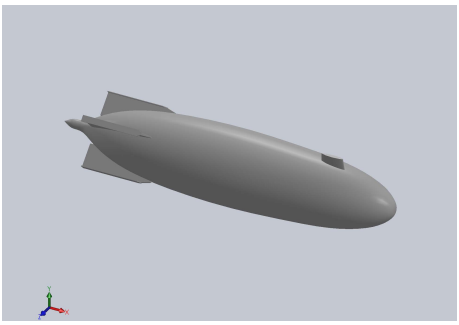 No-skates model	No-skates model: The skates are removed to understand the stability in the presence of the remaining appendages.
Design 5b	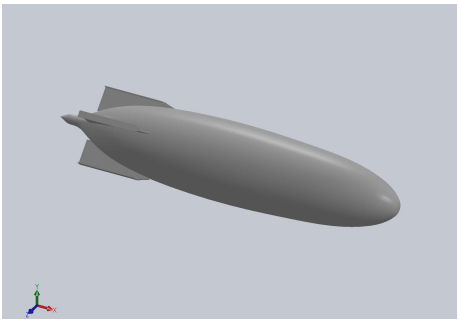 No-appendages model	No-appendages model: The sail and skates are removed to understand the stability in the presence of the remaining appendages.

Table 4. *Cont.*

Design Number	CAD Image	Description
Design 6	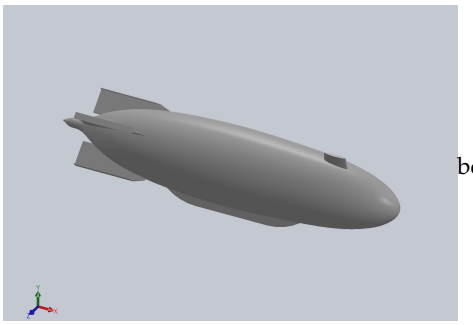 T-Strakes Extended model	T-strakes extended model: The fins have been extended beyond those of the hybrid narrow model in the lengthwise dimension.
Design 7	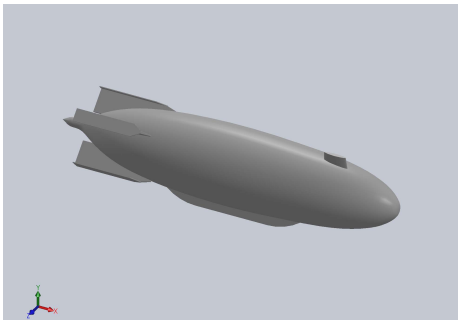 Hybrid Wide model	Hybrid wide model: This model based on Design 5 and Design 6 has wider T-edges on the strakes to increase surface area and mass for the stern.
Design 7.5a	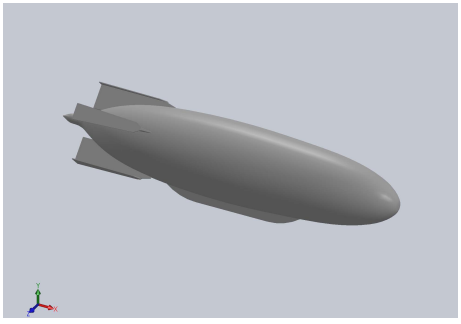 No-sail model	No-sail model: No sail in the hybrid trapezoidal model. This model is a step before Design 8, the only difference being the triangular leading edge of the T strakes.
Design 7.5b	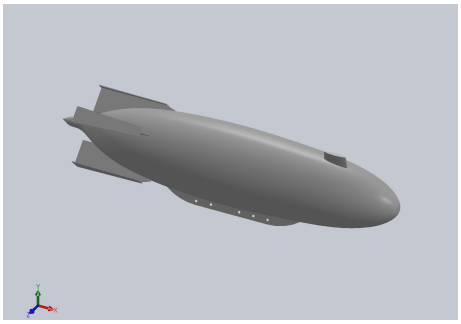 Equal holes model	Equal holes model: Equally spaced holes of the same diameter placed along the skates.

Table 4. *Cont.*

Design Number	CAD Image	Description
Design 7.5c	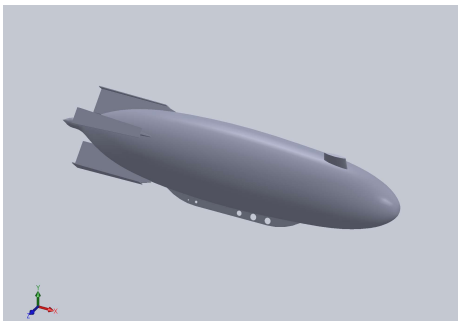 Unequal holes model	Unequal holes model: Holes of unequal diameter, evenly spaced, placed along the skates.
Design 7.5d	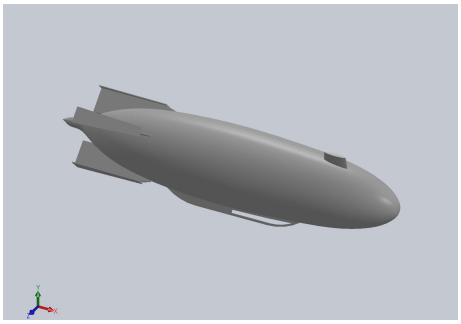 Slots model	Slots model: Slot cut out in the front part of the skates, removing most material after Design 7.5a.
Design 8	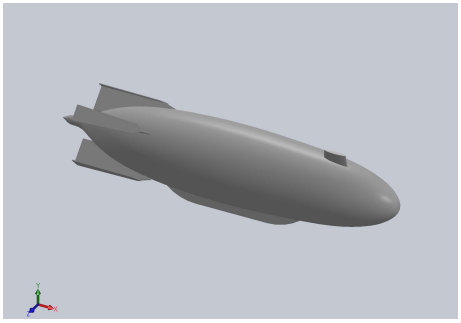 Hybrid triangle model	Hybrid triangle model: The fins are extended and have T-shaped edges. The edge is shaped with a triangular leading edge and taper leading to its widest trailing edge.

Table 5. Dimensions for the DIVE craft.

Parameter	Value
Length	L
Diameter	0.224 L
Volume	0.0284 L^3
Wetted Surface Area	0.571 L^2
Cruise Speed	4 kn
C_B C_G	0.0416 D

The drag of the craft is affected as design iterations are performed for stability. The increase in drag due to design variation is presented in Table 6.

Table 6. Value of drag coefficient, normalized using the WSA for select designs.

Design	C_d
Baseline	0.0608
Hybrid wide T	0.0879
Hybrid wide triangle	0.0878

5. Iterative Design Process

In the vertical plane, the stability desired is typically high. The G_V and $G_{V_{grav}}$ of the baseline design are calculated and presented in Figure 5. The negative value clearly indicates a concern in the vertical plane based on Table 2 that shows the range of G_V needed. The baseline design has a negative value of stability index G_V (i.e., dynamically unstable) to start with. While a controller may still be able to control the craft in its current state, design iterations were performed to increase its dynamic stability, primarily in the vertical plane. Moreover, the design of the control surfaces and their position on the hull causes concern regarding effectiveness of fins for control. The iterative process to increase the stability of the craft is performed through various design modifications shown in Table 4. The objective of the first few iterations was to increase the fixed and moving fin wetted surface area (WSA). However, other design constraints require that the craft diameter not exceed a specific diameter. Thus, T surfaces were added on the fins to further increase the WSA. The shape of the T surfaces was modified to make them as drag-optimized as conceptually possible. The modifications on the skates and sail were performed to understand their effect on stability. The additional design modifications on the skates were a way of removing material in the fore rather than adding material in the stern. The skates are not intended for controlling the craft and hence offer more design space to modify. The hydrodynamic coefficients of the main designs are non-dimensionalized according to the usual convention Feldman [5] and presented in Table 7.

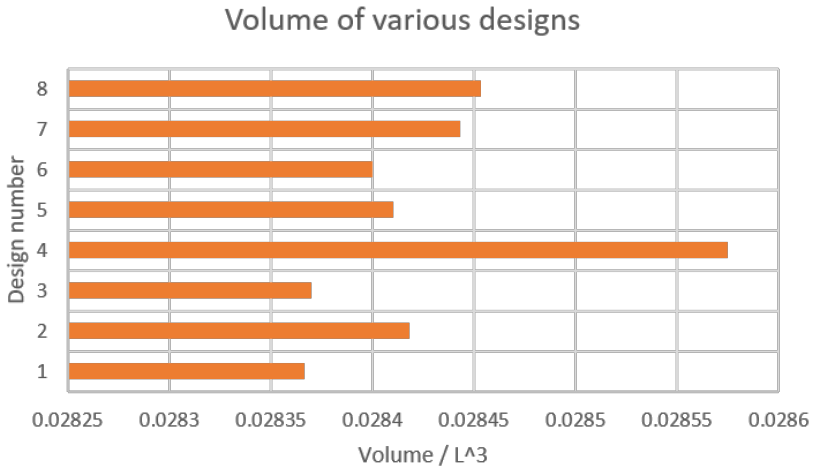

Figure 5. Non-dimensional volume for major designs.

Table 7. Absolute values of non-dimensional hydrodynamic coefficients for Design 1 (Table 4) are presented. Percentage changes of these coefficients with respect to Design 1 for the various design iterations for pure heave and pure pitch are presented.

Hydrodynamic Coefficients	Design 1	Design 2	Design 3	Design 4	Design 5	Design 6	Design 7	Design 8
M_{ww}	−0.0162	23.1	−108	−32.4	−65.6	−123	−93.3	−79.3
M_{uw}	0.0367	1.47	−8.82	2.12	−7.61	−20	−21.3	−22
$M_{\dot{w}}$	−0.000673	40.1	56.6	−7.41	56.4	102	172	132
Z_{ww}	−0.0236	16.5	−67.2	−23.4	−37.8	−90.3	−66.9	−53.5
Z_{uw}	−0.0233	1.69	19.9	−4.44	21.8	49.4	52.4	55.7
$Z_{\dot{w}}$	−0.0259	1.68	1.16	−0.066	2.2	3.62	4.85	4.84
M_{qq}	−0.00573	74.5	−47.1	−12.7	−22.8	−43.7	−19.2	−14.2
M_{uq}	−0.00266	33.6	46.5	8.6	70.8	69.3	101	107
$M_{\dot{q}}$	−0.00105	11	6.02	0.816	11.8	11.8	20.1	20.7
Z_{qq}	−0.014	72.9	−49	−8.53	−25.2	−48.4	−25.2	−19.4
Z_{uq}	−0.00532	47.4	68.3	7.76	98.9	103	150	155
$Z_{\dot{q}}$	−0.000218	109	110	−1.9	135	144	283	240

6. Results

6.1. Stability Indices

The intent of this iterative process is to increase the initial dynamic stability of the craft in the vertical plane of the craft. The lack of stability can be understood through the position of neutral and critical points for the craft Spencer [14]. Table 8 presents a comparison of various designs in terms of the NP and CP. Approaching the design differences from the perspective of the NP and CP, we note that the baseline design has an NP that is far from the COB, ahead of the bow of the craft as presented in Table 8. Similarly the CP is too far behind the COB in comparison to recommended positions. The recommended position of the NP is one third of the length of the craft, aft of the bow, and that of CP would be slightly aft of the NP at a moderate speed as shown by Spencer [14]. Design 1 (Table 4) with the two centers too far apart shows that the craft would have less control using the control fins to maneuver in the vertical plane. It would be difficult to maintain a constant depth during maneuvering since the moment arm from the CP is larger than desirable. As stability is increased, it is seen to move fore consistently. It is observed in Design 4 (Table 4) where the stability decreases, and the CP moves further aft, more so than Design 1 (Table 4). This is correlated by the fact that both stability indices G_V and G_{Vgrav} show that Design 4 is low in stability. The reason Design 4 remains above Design 1 in the stability trend is due to the presence of an additional stern appendage leading to higher surface area and hence more lift capacity at stern. This result may have differed if this appendage was placed in the horizontal plane, increasing its effective area and hence the stability.

Similarly, the NP, recommended to be maintained at one third of the length of the craft Spencer [14] from the bow, is seen to be much too fore, past the bow of the craft until the iterations approach Design 5 (Table 4). In Design 6 (Table 4), the NP is located closer to the ideal position. Understanding these observations summarized in Figure 6 shows that G_{Vgrav} captures this trend of NP and CP differences. Figure 7 shows the main coefficients that contribute in the value of G_V and G_{Vgrav} for each design. Between Designs 6 (Table 4) and 7 (Table 4), G_{Vgrav} shows a sign change. But G_V shows a sign change only after Design 7 (Table 4). This indicates that the definitions of CP (25) and NP (24) are both reflected in G_{Vgrav} at lower speeds with the inclusion of the hydrostatic term as opposed to G_V that does not include the definition of CP. Thus the index G_{Vgrav} indicates the marginal stability of a design that would otherwise be considered unstable.

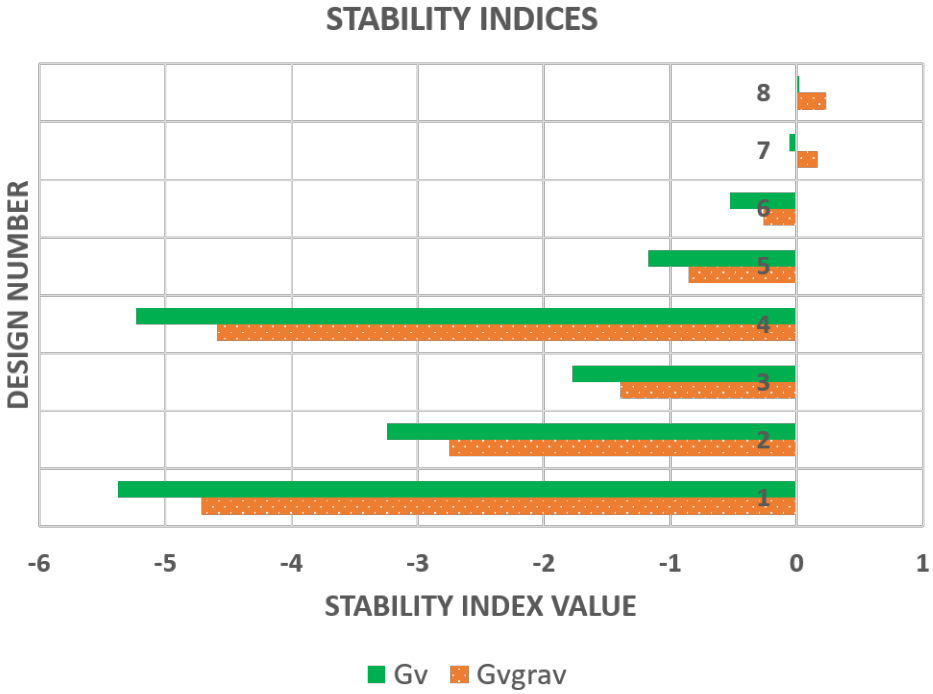

Figure 6. Stability indices for all major designs from least to most stable design.

Figure 6 shows the comparison of the stability index G_V for the various designs.

Table 8. The distance non-dimensionalized by L for the neutral and critical point along the center line from the origin or center of gravity.

Hydroplanes	Design 1	Design 2	Design 3	Design 4	Design 5	Design 6	Design 7	Design 8
neutral point at 4 kn	−0.765	−0.763	−0.581	−0.817	−0.580	−0.409	−0.395	−0.383
critical point at 4 kn	0.625	0.626	0.465	0.672	0.466	0.316	0.303	0.293

The main observation is that the increase in displacement and WSA at the stern of the craft considerably increases the stability of the craft, i.e, lift is generated at the stern of the craft. It is seen that the hydrodynamic coefficients M_{uw} and Z_{uq} follow similar trends with respect to each other except in Designs 6 (Table 4) and 3 (Table 4). These two coefficients are the main contributors to the stability index apart from the inertia term. They indicate the trends of pitching moment and heave force respectively as reactions to external forces along axes Z and Y.

In the designs with extended fins and strakes, such as Design 2 (Table 4), there is a 45% increase in stability index G_V. This correlates with the fact that there is an increased volume in the stern as shown in Figure 5. This shows that the increase in mass and area in the stern has a positive effect on stability for this craft. The extension of fins in the lengthwise dimension was not preferred or pursued since the propeller inflow would be affected. This led to attempts in increasing the effective area through adding T-shaped edges to the fixed and moving fins in Design 3 (Table 4) and Design 8 (Table 4). Design 4 (Table 4) showing a lower stability index than that of Designs 2 (Table 4) and Design 3 (Table 4) indicates that the presence of the fins in the horizontal plane would have increased the stability index in the vertical plane. Thus, a change in surface area of stern appendages was needed, not only in terms of magnitude but also in position. The position of appendages need modification to avoid flow stagnation near the moving fins. While most of the trend of G_{Vgrav} is captured by both indices, the sign change and magnitude of the stability index varies between the two. G_{Vgrav} indicates that the hydrostatic term has a positive effect on stability at low-moderate speeds.

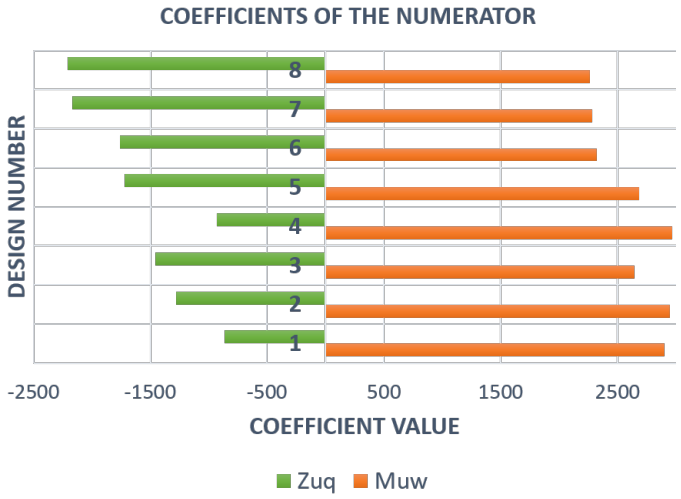

Figure 7. Absolute value of hydrodynamic coefficients contributing to the numerator of the term stability index G_V to indicate the main contributors to stability change apart from the mass term.

Designs 7 (Table 4) and 8 (Table 4) are pretty close to each other in concept, differing in the shape of the T edges to facilitate better drag and flow characteristics. It is important to note that though the values of G_{Vgrav} and G_V for Design 8 indicate stability according to Table 2, Section 2.2 indicates a marginal stability with G_{Vgrav} and minimal stability with G_V. Thus, while G_V indicates an increase of stability from Design 7 (Table 4) to 8 (Table 4), with a sign change and about 140%, G_{Vgrav} indicates a more realistic increase within the same sign of 43% upon considering the hydrostatic restoring force. Design iterations were paused at Design 8 to include another amplitude of VPMM and implement the LPM for the numerical observation of the increase in stability. Now that G_{Vgrav}> 0.2, this model is considered marginally stable.

Designs 5 (Table 4), 6 (Table 4), and 7 (Table 4) show a progressive increase in G_{Vgrav} and G_{Vgrav}. The magnitude of increase in G_V is high enough to warrant investigation of the true magnitude of increase in stability. While the authors recognize that the nature of the stability index G_V is applicable only at the beginning of the maneuver, the inclusion of the hydrostatic term in the index G_{Vgrav} becomes imperative since the effect of gravity becomes important in design iterations with mass changes.

It is also noted that G_V and G_{Vgrav} follow the same overall trend and are of the same signage for all the designs considered except Design 7 (Table 4). This can be attributed to the position of CP as explained earlier in this section. This also implies that Design 7 (Table 4) and Design 8 (Table 4) would have been discarded if G_V was used at this speed instead of G_{Vgrav}. This becomes relevant for the size and speed of underwater vehicles being developed in today's market.

Overall, it is noted that there is an increase of 100% stability in G_V and a 105% increase in G_{Vgrav} with an increase in drag of 16% (between Designs 1 and 8).

6.2. Investigation of the Sail

Considering the design of the DIVE craft, the asymmetry in the vertical plane leads to questions concerning which of the appendages have the most effect on stability. During the iteration of Design 5 (Table 4), simulations with Models 5a (Table 4) and 5b (Table 4) were performed. Figure 8 indicates that there is a reduction in stability due to the removal of either appendage. This indicates that the increase in WSA in the fore-body plays a large role in the magnitude of stability, as expected. Figure 9 further validates the increase of WSA and volume. There is no noteworthy difference in the trends of G_V and G_{Vgrav} in this regard except the known and increased value of stability shown by G_{Vgrav} for each design.

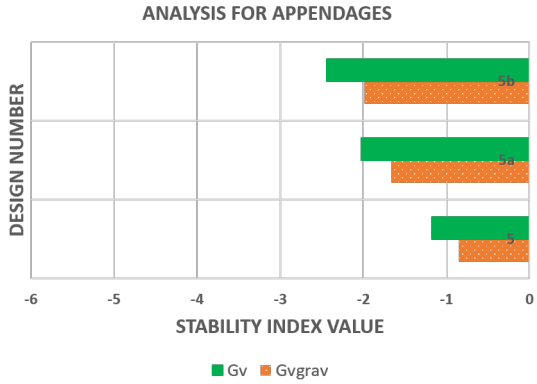

Figure 8. Stability indices for sail contribution.

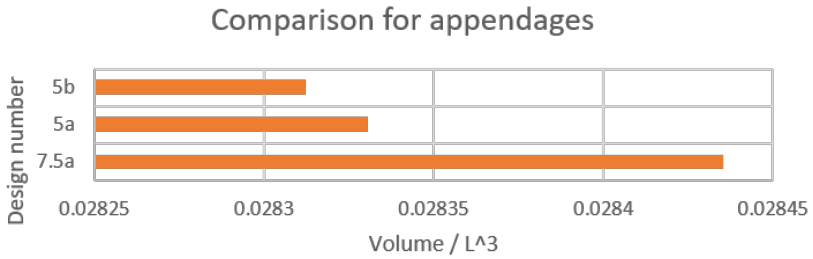

Figure 9. Value of non-dimensional volume for designs with appendage modification.

6.3. Investigation of the Skates

The skates are modified to remove area from them in different ways to understand if the stability could be improved. The Designs 7.5a,b,c, and d (Table 4) are a step prior to Design 8, exploring the modification of skates. The entire removal of skates with the sail remaining on the craft in Design 7.5a in Figure 10 shows that both G_{Vgrav} and G_V are the least in this configuration in comparison to other modifications of the skates. This shows that the removal of material is conducive to a stability increase only when decreasing the volume in the fore, as opposed to both stern and fore. In other words, the ratio of mass in the stern vs. mass in the fore needed to be increased. Hence, the holes/slot in the skates were cut out to remove material from the fore of the craft. This was viewed as an alternative to adding material to the stern, since almost half of the skates extend to the fore, past the center of gravity of the craft. It is noted that the presence of equally sized and positioned holes across the skates leads to a higher stability. The removal of material from the skates leading to a slight reduction in volume from Design 1 (Table 4) as illustrated in Figures 5 and 11 has a significant effect on G_{Vgrav}. Design 7.5d with slots cut out has the most stability within the modified designs as shown in in Figure 10. Therefore, the designs with holes are all minimally stable. G_V indicates all four modified designs to be unstable with negative values. This effort is a clear indication of the hydrostatic term and its effect on stability due to change in mass.

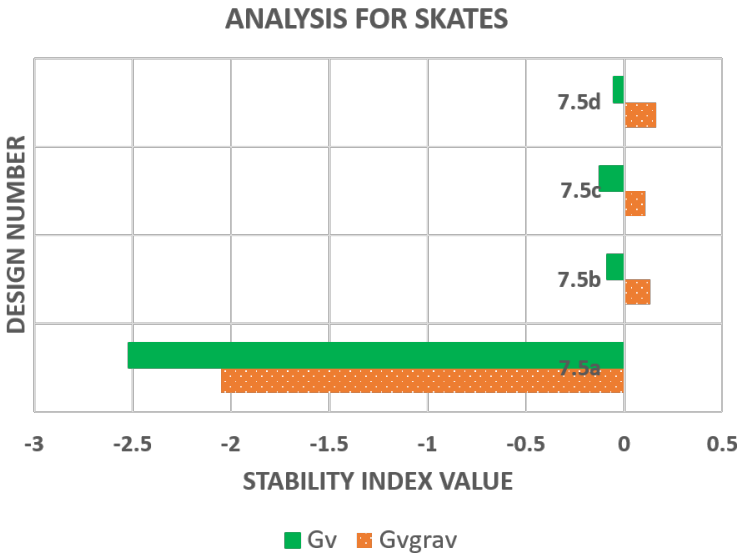

Figure 10. Stability indices for skate modification designs.

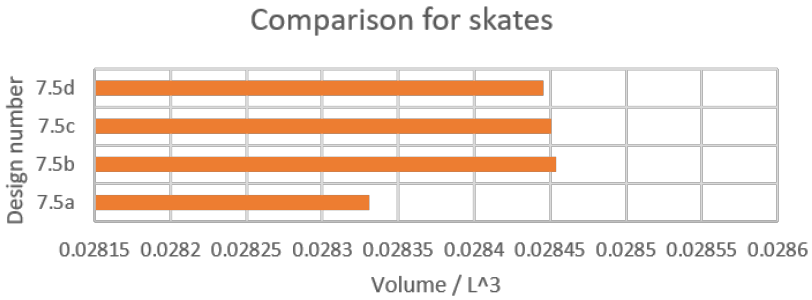

Figure 11. Value of non-dimensional volume for designs with skate modification.

7. Assessment of Implications of Stability Analysis

7.1. Pitching/Yawing Maneuver for the Vertical and Horizontal Planes for Verification of Stability

A numerical lumped parameter model with 6 DOF was chosen to implement the hydrodynamic coefficients and simulate a simple pitching maneuver without a controller. The initial conditions of the craft are set to neutral buoyancy and a uniform advance motion of no attitude except a pitch of 0.6°. The C_BC_G is set to 0.04D. The vertical plane motions are locked for the horizontal plane maneuver and vice versa. This maneuver was attempted on Design 8 (Table 4) and Design 1 (Table 4) to compare the stability of the craft in the vertical plane. It is observed that the the maneuver results in a certain number of oscillations in both the designs. These oscillations damp out in Design 8 but remain in Design 1, indicating that Design 1 is unstable and Design 8 is marginally stable. The amplitude of oscillations is observed to be higher for Design 1, indicating that the craft struggles to recover from the initial perturbance. Figures 12 and 13 show the output of this maneuver in the vertical plane for the baseline design and hybrid triangle design, respectively. In the horizontal plane, both craft are able to perform the yaw maneuver without oscillations.

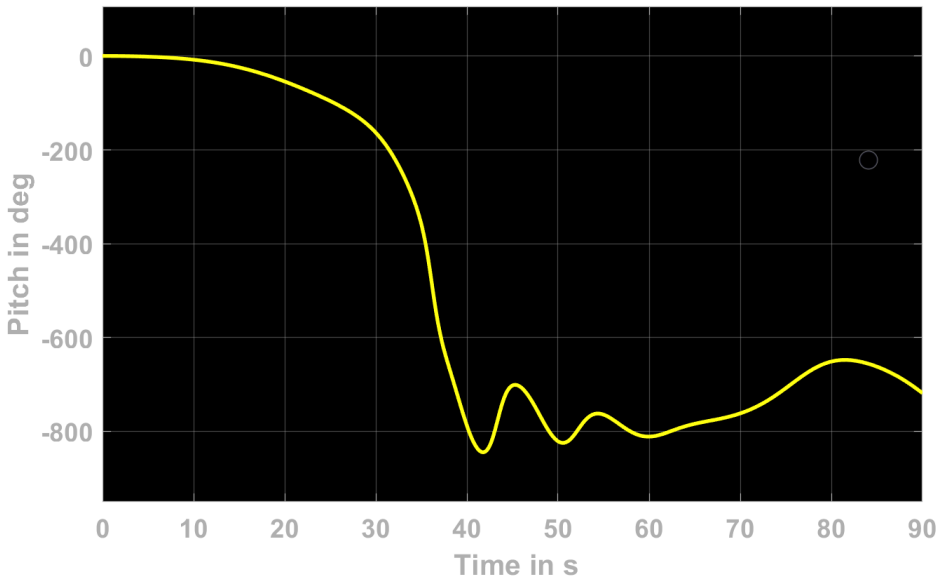

Figure 12. Dynamics in the vertical plane predicted by the LPM for the baseline: pitch output of the craft vs. time.

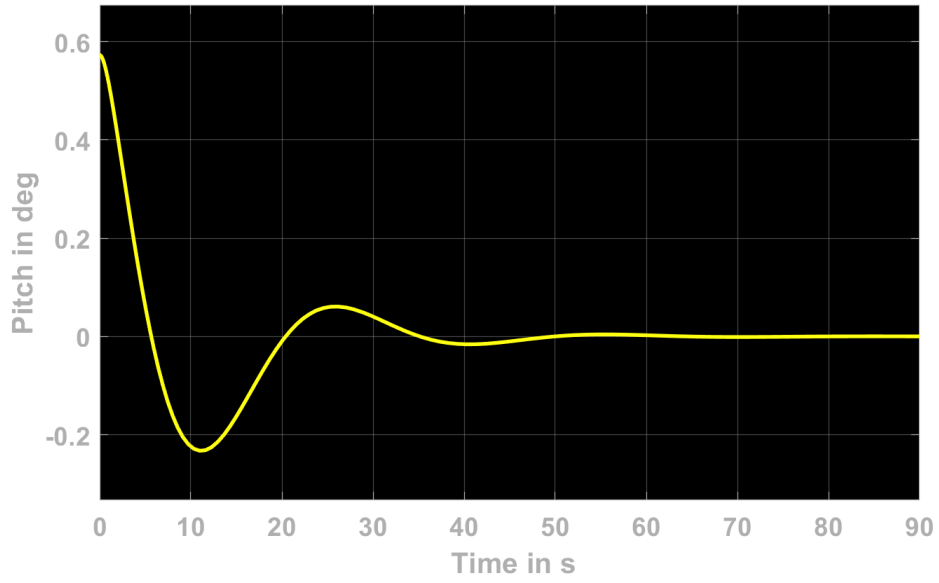

Figure 13. Dynamics in the vertical plane predicted by the LPM for the hybrid triangle design: pitch output of the craft vs. time.

7.2. Circular Maneuver for CFD Validation of Stability

Going a step further from the LPM, both Designs 1 and 8 are implemented in CFD to perform the turning circle maneuver. The turn-circle maneuver is a traditional maneuver used in marine craft to obtain the turn-circle radii at various different angles of rudder deflection to understand the maneuverability and stability in the horizontal plane. This is achieved at 10° and 20° rudder deflections for Designs 1 and 8. The results in Table 9 show that that Design 1 makes a tighter turn resulting in smaller radii than Design 8 at both rudder angles. This validates the fact that Design 8 is more stable and hence less maneuverable than Design 1, achieving the main goal of this research effort.

Table 9. Turning circle maneuver: steady turning diameter for the most and least stable models through implementation of LPM.

Rudder Deflection [°]	Hybrid Triangle [m]	Baseline [m]
10	6.2 L	3.4 L
20	3.3 L	2.3 L

8. Closing Remarks and Future Work

The research effort presented in this paper is mainly to calculate, validate, and improve the stability of the hydrodynamic design of a drag-optimized underwater vehicle, along with the implementation of a stability index in the vertical plane. The effects of the control system are out of scope for this research. This effort serves an example of the hydrostatic term being needed for the assessment of the dynamic stability in the vertical plane in a proper range of low speeds, as, for instance, indicated in Figure 3 for this particular case. It is important to note that the new stability index, $G_{V_{grav}}$, which includes the effect of gravity, highlights the hydrostatic term. Future work shall include implementation of asymmetric coefficients for better resolution of vertical plane stability. Moreover, the proposed new index could encompass the definition of another non-dimensional parameter to include the effect of the control authority in the definition of the dynamic stability characteristic. The effective area of control surfaces could be analyzed in correlation to stability indices to form the basis of a design guideline. The improvement of the numerical dynamic model, particularly with regard to the efficient and accurate estimation of lumped parameters from simulated maneuvers by CFD, is another avenue for future work.

Author Contributions: L.M.: concept, technical recommendations, draft preparation; S.B.: concept, technical recommendations, draft preparation; D.J.S.: technical recommendations, draft preparation. All authors have read and agreed to the published version of the manuscript.

Funding: This study was primarily funded by Dive Technologies with partial contribution from ONR, grants N00014-19-1-2507 and N0001-20-1-2621.

Institutional Review Board Statement: Not applicable.

Informed Consent Statement: Not applicable.

Conflicts of Interest: The authors declare no conflict of interest.

References

1. Minnick, L. A Parametric Model for Predicting Submarine Dynamic Stability in Early Stage Design. Ph.D. Thesis, Virginia State and Polytechnical University, Blacksburg, VA, USA, 2006.
2. Sweat, C.W. *Hydrodynamic Stability Criteria for Adequate Torpedo Stability And Response*; Technical Report; Department of the Navy: China lake, CA, USA, 1958. .
3. Lambert, J. *The Effect of Changes in the Stability Derivatives on the Dynamic Behaviour of a Torpedo*; Technical Report; Admiralty Research Laboratory: London, UK, 1956.
4. Lewis, E.V.; Society of Naval Architects and Marine Engineers (U.S. *Principles of Naval Architecture: Motions in Waves and Controllability*; Principles of Naval Architecture, Society of Naval Architects and Marine Engineers: Jersey City, NJ, USA, 1988.
5. Feldman, J. *Method of Performing Captive-Model Experiments to Predict The Stability and Control Characteristics of Submarines*; Technical Report June; Naval Surface Warfare Center: Bethesda, MD, USA, 1995.
6. Roddy, R.F. *Investigation of the Stability and Control Characteristics of Several Configurations of the DARPA SUBOFF Model from Captive-Model Experiments*; Technical Report; David Taylor Research Center: Bethesda, MD, USA, 1990.
7. Renilson, M. *Submarine Hydrodynamics*, 2nd ed.; Springer International Publishing: Berlin/Heidelberg, Germany, 2015; Volume 33, pp. 137–138. [CrossRef]
8. Park, J.Y.; Kim, N.; Shin, Y.K. Experimental study on hydrodynamic coefficients for high-incidence-angle maneuver of a submarine. *Int. J. Nav. Archit. Ocean. Eng.* **2017**, *9*, 100–113. [CrossRef]
9. Feldman, J. *Revised Standard Submarine Equations of Motion*; Technical Report June; David W. Taylor Naval Ship Research and Development Center: Bethesda, MD, USA, 1979.
10. Fossen, T.I. Hydrostatics. In *Handbook of Marine Craft Hydrodynamics and Motion Control*; John Wiley & Sons, Ltd.: Hoboken, NJ, USA, 2011; Chapter 4, pp. 59–80. [CrossRef]

11. Coe, R.; Neu, W. Virtual Planar Motion Mechanism tests in a CFD environment. In Proceedings of the Virginia Space Grant Consortium Student Research Conference, 2012. Available online: https://vsgc.odu.edu/studentresearchconference/ (accessed on 15 January 2021)
12. Cho, Y.J.; Seok, W.; Cheon, K.H.; Rhee, S.H. Maneuvering simulation of an X-plane submarine using computational fluid dynamics. *Int. J. Nav. Archit. Ocean. Eng.* **2020**, *12*, 843–855. [CrossRef]
13. Lewandowski, E.M. *The Dynamics of Marine Craft Maneuvering and Seakeeping*; World Scientific: Singapore, 2004.
14. Spencer, J. Stability and Control of Submarines. *J. R. Nav. Sci. Serv.* **1980**, *23*, 187–205.
15. Ogata, K. *Modern Control Engineering*; Prentice Hall: Upper Saddle River, NJ, USA, 2010.
16. Bottacini, M. *The Stability Coefficients of Standard Torpedos*; Technical Report; Underwater Ordinance Department: China Lake, CA, USA, 1954.
17. Njaka, T.; Miller, L.M.; Brizzolara, S.; Stilwell, D.J. Method for Improving Existing Maneuvering Models to Accomodate Large Drift Angles. In Proceedings of the Global Virtual Oceans, Biloxi, MS, USA, 5–30 October 2020.
18. Dubbioso, G.; Muscari, R.; Ortolani, F.; Di Mascio, A. Analysis of propeller bearing loads by CFD. Part I: Straight ahead and steady turning maneuvers. *Ocean. Eng.* **2017**, *130*, 241–259. [CrossRef]